

A Comparative Analysis of Deep Reinforcement Learning-enabled Freeway Decision-making for Automated Vehicles

Teng Liu, Bing Huang, Xingyu Mu, Fuqing Zhao, Xiaolin Tang, Dongpu Cao

Abstract—Deep reinforcement learning (DRL) is becoming a prevalent and powerful methodology to address the artificial intelligent problems. Owing to its tremendous potentials in self-learning and self-improvement, DRL is broadly serviced in many research fields. This article conducted a comprehensive comparison of multiple DRL approaches on the freeway decision-making problem for autonomous vehicles. These techniques include the common deep Q learning (DQL), double DQL (DDQL), dueling DQL, and prioritized replay DQL. First, the reinforcement learning (RL) framework is introduced. As an extension, the implementations of the above mentioned DRL methods are established mathematically. Then, the freeway driving scenario for the automated vehicles is constructed, wherein the decision-making problem is transferred as a control optimization problem. Finally, a series of simulation experiments are achieved to evaluate the control performance of these DRL-enabled decision-making strategies. A comparative analysis is realized to connect the autonomous driving results with the learning characteristics of these DRL techniques.

Index Terms—Decision-making, deep reinforcement learning, autonomous vehicles, DQL, double DQL, dueling DQL, PR-DQL

NOMENCLATURE

HSM	Hierarchical State Machine
CTP	Critical Turning Point
POMDP	Partially Observable Markov Decision Process
DRL	Deep Reinforcement Learning
DL	Deep Learning
RL	Reinforcement Learning
DQL	deep Q learning
PPO	Proximal Policy Optimization
A3C	Asynchronous Advantage Actor-Critic
IDM	Intelligent Driver Model

This work was in part supported by the State Key Laboratory of Mechanical System and Vibration (Grant No. MSV202016). (Corresponding authors: F. Zhao and X. Tang)

T. Liu is with Department of Automotive Engineering, Chongqing University, Chongqing 400044, China, and also with Department of Mechanical and Mechatronics Engineering, University of Waterloo, N2L 3G1, Canada. (email: tengliu17@gmail.com)

B. Huang, X. Mu, and X. Tang are with College of Automotive Engineering, Chongqing University, Chongqing, 400044, China. (email: 20162361@cqu.edu.cn, 20162364@cqu.edu.cn, tangxl0923@cqu.edu.cn)

F. Zhao is with the Comprehensive test center, Chongqing Institute of Green and Intelligent Technology, Chinese Academy of Science, 400714, China. (jeff8952260@gmail.com)

D. Cao is with the Department of Mechanical and Mechatronics Engineering, University of Waterloo, N2L 3G1, Canada. (email: dongpu.cao@uwaterloo.ca)

MOBIL	Minimizing Overall Braking Induced by Lane Change
DDQL	double DQL
MDP	Markov decision process

I. INTRODUCTION

Autonomous driving becomes a hotspot recently for its tremendous potential to improve driving safety and efficiency [1]. With the development of artificial intelligence and communication science, great advances have been made on the four crucial components of an autonomous driving system. The four components are respectively perception, decision-making, planning, and control [2].

The Decision-making module is the brain of the autonomous driving system [3]. It has to generate suitable motion behaviors for specific missions in a dynamic and uncertain environment. Many researches have been done to enhance the ability of the decision-making module for autonomous driving. For example, Do, Q. H. et al. proposed a grid map to category the driving environment. To select suitable behavior for each category, the authors constructed a dx/dv graph based on real-world data [4]. In Ref. [5], Hierarchical State Machine (HSM) is utilized to solve the behavior decision-making problem for lane-changing in a predefined environment. Then, Shu, K. et al. proposed a hierarchical decision-making strategy for the left-turn at intersections. The high-level layer is for paths generation based on Critical Turning Point (CTP). In the low-level layer, the left planning problem is turned into a Partially Observable Markov Decision Process (POMDP) problem using the CTP concept [6]. Furthermore, the authors in [7] employed Mixed Observable Markov Decision Process to model the decision making for lane-changing, which considered the measurement and motion uncertainties.

Deep Reinforcement Learning (DRL) is regarded as a promising method for decision-making of autonomous driving. DRL combines the superior feature extraction ability of Deep Learning (DL) and the decision ability of Reinforcement Learning (RL) in sequential problems. For example, Mirchevska B et al. presented a DQL based approach for behavior decision-making for lane-changing in a simulated highway [8]. To guarantee safety, formal safety verification was defined. Ref. [9] proposed a hierarchical RL-based control architecture, which can generate safe and smooth trajectories without depending on large quantities of labeled driving data. Then, F. Ye et al. proposed Proximal Policy Optimization (PPO) based DRL for mandatory lane-changing, which can take appropriate actions at a rate of 95% in dense traffic [10]. In ref. [11], X. Feng et al. built a lane-changing strategy by DRL, including DQL and Asynchronous Advantage Actor-Critic

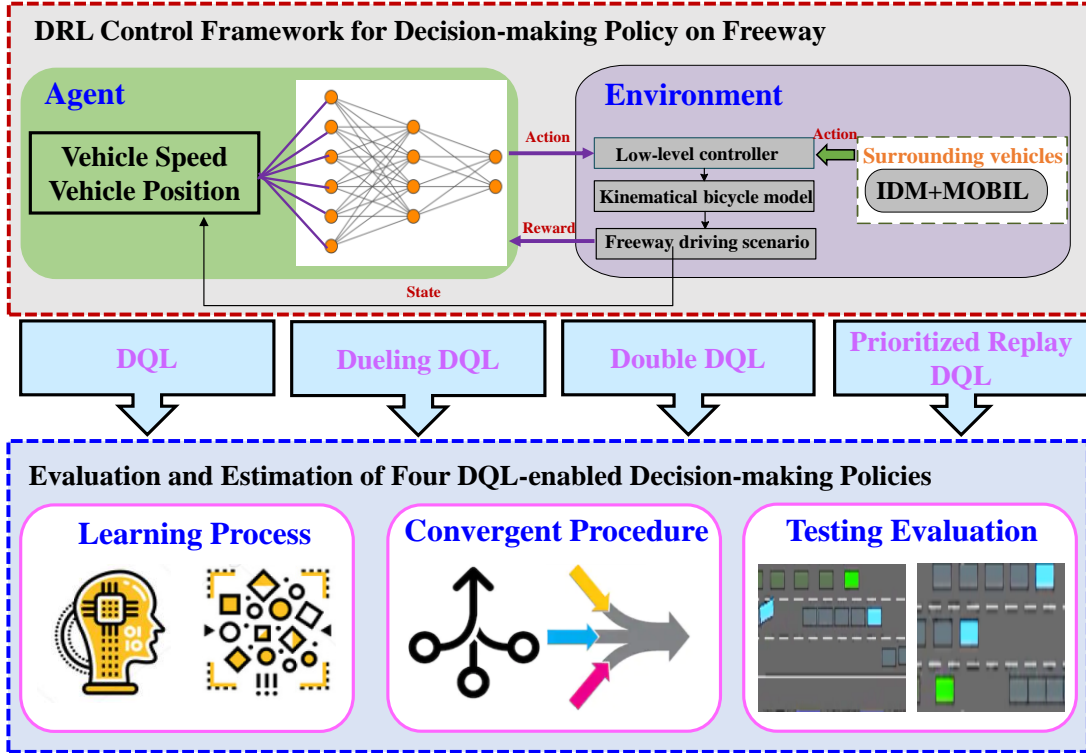


Fig. 1. Decision-making control framework based on four DQL algorithms for autonomous vehicles on freeway.

(A3C), and this strategy has a great generalized ability. To improve its performance, a new way to combine DRL agents is proposed. Until now, there is no comprehensive literature to compare the performance of different DRL methods on the freeway decision-making problem to our best knowledge.

In this paper, a comprehensive comparison of multiple DRL approaches on the freeway decision-making problem for autonomous vehicles is constructed, including DQL, DDQL, dueling DQL, and prioritized replay DQL, as depicted in Fig. 1. First, the RL framework and the DQL methods mentioned above are introduced. Then, the decision-making problem for the automated vehicles in the freeway driving scenario is constructed, wherein the surrounding vehicles follow the Intelligent Driver Model (IDM) and the Minimizing Overall Braking Induced by Lane Change (MOBIL) model. Finally, simulation experiments are achieved to discuss and analyze the control performance of these compared DRL-enabled decision-making strategies.

The potential contributions of this paper are outlined as follows: 1) a meticulous and comprehensive comparison is conducted for epidemic DRL techniques in decision-making problems on the freeway; 2) a theoretical and mathematic analysis is executed to build the DQL, DDQL, dueling DQL, and prioritized replay DQL algorithms; 3) a composite discussion and evaluation are depicted to elaborate the merits and demerits of disparate DRL-based decision-making policies. This work wants to be a guidance and layout to apply the DRL approaches into the freeway decision-making problems for autonomous vehicles.

The construction of the following paper is depicted as follows: multiple DQL methods are introduced in Section 2. Sec-

tion 3 constructs the decision-making problem on the freeway. Experiment results are compared and analyzed in Section 4. Section 5 concludes the paper.

II. INTRODUCTION OF MULTIPLE DQL METHODS

This section introduces various DRL methods. Firstly, the Markov decision process and the interaction between agent and environment in RL are explained. Then, Common DQL is introduced, which combines a neural network and a Q-learning algorithm. Finally, three improved versions of DQL are introduced separately, which are Double DQL, Dueling DQL, and Prioritized Replay DQL.

A. Preliminaries of RL

Solving the RL problem can be understood as how to maximize the cumulative reward of the agent in the process of interaction with the environment [12-15]. When the environment is completely observable, individuals can construct a Markov decision process (MDP) to describe the whole reinforcement learning problem. Sometimes the environment is not completely observable, so individuals can construct an approximate fully observable environment description based on their historical observation data. So it can be said that almost all RL problems can be transformed into MDPs [16-18].

In the highway decision-making problem, the agent is the ego vehicle, while the environment is the surrounding vehicles (including driving conditions). Markov property means that every state in the process has Markov property, that is, the state variable at the next moment is only related to the current state and has nothing to do with the state at the previous time [19]. MDPs are based on Markov property and consider the feedback

of state transition and the choice of individual behavior. MDP can represent RL problems as tuples (S, A, P, R, γ) , where S and A are state sets and action sets. P is the core of RL, which represents the state transition model based on behavior, while R represents the reward model based on state and behavior. Because the future reward is not as important as the present reward, γ is introduced as the discount rate to show the importance of future reward.

The cumulative return R reflects the sum of future rewards, and can be calculated as follows:

$$R = \sum_{t=0}^K \gamma^t r_t \quad (1)$$

where t is the discrete-time steps to make control decisions in an episode, and r_t indicates the relevant reward. K is the time-step of the end of the environment, which could be ∞ .

Value functions could be used to learn policies. These functions can calculate the expectation of R under a given strategy. Two value functions are defined based on the state s and state-action pair (s, a) as:

$$V^\pi(s) = E_\pi \left[\sum_{t=0}^K \gamma^t r_t \mid s_{t=0} = s \right] \quad (2)$$

$$Q^\pi(s, a) = E_\pi \left[\sum_{t=0}^K \gamma^t r_t \mid s_{t=0} = s, a_{k=0} = a \right] \quad (3)$$

where π is the policy, V is the state value function, and Q is the state-action value function. The state-action function can also be written in another recursive form:

$$Q^\pi(s, a) = E_\pi \left[r_t + \gamma \max_{a'} Q^\pi(s', a') \right] \quad (4)$$

where s' and a' are the state and action at the next time step.

Finally, select the action that could get the highest expected return value as the optimal control policy by using the state-action value function.

$$\pi(s) = \arg \max_a Q(s, a) \quad (5)$$

B. Common DQL

DQL combines Q-learning with deep learning and uses a neural network to estimate Q value. In the common Q-learning, the recursive form of the state-action function is shown below:

$$Q(s, a) \leftarrow Q(s, a) + \alpha [r + \gamma \max_{a'} Q(s', a') - Q(s, a)] \quad (6)$$

where α is named as the learning rate.

When dealing with multiple state and action variables, the Common Q-learning needs much time to calculate the mutable Q table. DQL solves this problem well and uses a neural network to express the Q table as $Q(s, a; \theta)$, in which θ is the parameters of the neural network. The primary purpose of the DQL method is to train these parameters accurately.

Q-learning uses ϵ -greedy policy to generate actions. The final strategy to generate behavior and the strategy for evaluation can be different, which is called the Off-Policy method. DQL is also an Off-Policy algorithm, but the difference is that

the Q-learning has only one neural network to calculate target and predicted value in Q-learning, while DQL has two networks, prediction network, and the target network. The target network has the same structure as the prediction network, but the prediction network is updated every iteration, while the target network would copy the parameters from the prediction network every specified number of time steps.

In order to reflect the difference between the approximate Q table and the actual Q table in DQL, the loss function is introduced as follows:

$$L(\theta) = E \left[\sum_{t=1}^N (y_t - Q(s, a; \theta))^2 \right] \quad (7)$$

where

$$y_t = r_t + \gamma \max_{a'} Q(s', a'; \theta') \quad (8)$$

The θ and θ' represent the parameters of the prediction network and target network, respectively.

The neural network uses a gradient descent method to update iteratively in DQL, and the gradient formula is as follows:

$$\nabla_\theta L(\theta) = E[(y_t - Q(s, a; \theta)) \nabla_\theta Q(s, a; \theta)] \quad (9)$$

In addition, DQL also uses the experience replay method [20]. Due to the strong correlation between samples, it is inefficient to learn directly from continuous samples. The method of experience replay is used to randomize the samples so as to break the correlations and improve the learning efficiency. The Common DQL algorithm is presented in Table I, and the function Φ denotes that a fixed representation length of histories is used as the input of the neural network.

TABLE I
IMPLEMENTATION CODE OF COMMON DQL ALGORITHM

Common DQL Algorithm

1. Initialize replay memory D to capacity N
2. Initialize action-value function Q with random weights
3. **For** episode = 1, 2, ..., M **do**
4. Initialize state s_1 and preprocessed sequenced Φ_1
5. **For** $t = 1, 2, \dots, T$ **do**
6. With probability ϵ select a random action a_t
otherwise select $a_t = \max_a Q(\Phi(s_t), a; \theta)$
7. Execute action at in emulator and observe reward r_t and image x_{t+1}
8. Set $s_{t+1} = s_t, a_t, x_{t+1}$ and preprocess $\Phi_{t+1} = \Phi(s_{t+1})$
9. Store transition $(\Phi_t, a_t, r_t, \Phi_{t+1})$ in D
10. Sample random minibatch of transitions $(\Phi_j, a_j, r_j, \Phi_{j+1})$ from D
11. Set $y_j = r_j$ for terminal Φ_{j+1}
otherwise set $y_j = r_j + \gamma \max_{a'} Q(\Phi_{j+1}, a'; \theta)$
12. Perform a gradient descent step on $(y_j - Q(\Phi_j, a_j; \theta))^2$ according to equation 9
13. **end for**
14. **end for**

C. Double DQL

Common Q-learning and DQL use max operator to evaluate the value function and select the action. This way of overoptimistic selection leads to an overestimation of value [21]. In

order to prevent this, we can use two different value functions to decouple the selection from the evaluation. So in Double DQL (DDQL), the max operation is decomposed into action selection and action evaluation.

DQL itself has two neural networks, prediction network, and target network, so we do not need to introduce other networks in DDQL. In addition to the calculation method of the target y_t , the algorithm flow of the Double DQL algorithm and Common DQL algorithm is exactly the same. y_t in Double DQL is expressed as follows:

$$y_t^{DoubleDQL} = r_t + \gamma Q(s', \arg \max_{a'} Q(s', a'; \theta), \theta') \quad (10)$$

Therefore, we can evaluate the greedy strategy according to the prediction network, and use the target network to estimate its value. This Double DQL algorithm can effectively reduce the overestimation of values. The realization procedure of Double DQL is displayed in Table II.

TABLE II
IMPLEMENTATION CODE OF DOUBLE DQL ALGORITHM

Double DQL Algorithm

1. Input: target network replacement frequency N'
2. Initialize replay memory D to capacity N
3. Initialize action-value function Q with random weights
4. **For** episode = 1, 2, ..., M **do**
5. Initialize state s_1 and preprocessed sequenced Φ_1
6. **For** $t = 1, 2, \dots, T$ **do**
7. With probability ϵ select a random action a_t
otherwise select $a_t = \max_a Q(\Phi(s_t), a; \theta)$
8. Execute action at in emulator and observe reward r_t
and image x_{t+1}
9. Set $s_{t+1} = s_t, a_t, x_{t+1}$ and preprocess $\Phi_{t+1} = \Phi(s_{t+1})$
10. Store transition $(\Phi_t, a_t, r_t, \Phi_{t+1})$ in D
11. Sample random minibatch of transitions $(\Phi_j, a_j, r_j, \Phi_{j+1})$
from D
12. Set $y_j = r_j$ for terminal Φ_{j+1} ,
otherwise set $y_j = r_j + \gamma Q(\Phi_{j+1}, \arg \max_{a'} Q(\Phi_{j+1}, a'; \theta); \theta')$
13. Perform a gradient descent step on $(y_j - Q(\Phi_j, a_j; \theta))^2$
according to equation 9
14. Replace target parameters θ by θ' every N' steps
15. **end for**
16. **end for**

D. Dueling DQL

In some RL cases, there may be a certain state that no matter what action is taken, the state at the next moment will not be greatly affected. For example, when there is no car in front of the agent on the highway, the selection of action will not affect the driving state. Therefore, the state-action function is decomposed into state-value function $V(s)$ and the advantage function $A(s, a)$ in Dueling DQL, which can better describe the process of reinforcement learning. The expression is as follows:

$$Q^\pi(s, a) = A^\pi(s, a) + V^\pi(s) \quad (11)$$

Unlike the Common DQL, a stream of two fully connected layers is used in Dueling DQL instead of following the convolutional layers with a sequence of fully connected layers.

This structure of the network makes it possible to estimate the value and advantage functions separately. In the end, the single output of the Q function is generated by combining the two streams. The calculation of the state-action function with two parameters in the network is defined as follows:

$$Q^\pi(s, a; \theta, \beta_1, \beta_2) = V^\pi(s; \theta, \beta_1) + A^\pi(s, a; \theta, \beta_2) \quad (12)$$

where θ is the parameters of the convolutional layers, while β_1 and β_2 are the parameters of the two streams of fully-connected layers.

But (12) is unidentifiable, which means that we cannot recover V and A uniquely by given Q . In order to solve the problem of identifiability, we can force the advantage function estimator to have zero superiority in the selected actions [22]. So (12) can be rewritten as follows:

$$Q^\pi(s, a; \theta, \beta_1, \beta_2) = V^\pi(s; \theta, \beta_1) + (A^\pi(s, a; \theta, \beta_2) - \max_{a'} A^\pi(s, a'; \theta, \beta_2)) \quad (13)$$

$$a^* = \arg \max_{a'} Q(s, a; \theta, \beta_1, \beta_2) = \arg \max_{a'} A(s, a'; \theta, \beta_2) \quad (14)$$

By (13) and (14), we can obtain the following equation:

$$Q^\pi(s, a^*; \theta, \beta_1, \beta_2) = V^\pi(s; \theta, \beta_1) \quad (15)$$

Therefore, the rewritten equation (13) is identifiable. Meanwhile, because the architecture of the Dueling DQL has the same input-output interface as the Common DQL, it is easy to train the Dueling DQL through the learning algorithm with Q networks. The pseudo-code of Dueling DQL is shown in Table III, wherein the advantage network could estimate the worth of each chosen control action. This feature could improve the property of the obtained control policy.

TABLE III
IMPLEMENTATION CODE OF DUELING DQL ALGORITHM

Dueling DQL Algorithm

1. Initialize replay memory D to capacity N
2. Initialize action-value function Q with random weights
3. **For** episode = 1, 2, ..., M **do**
4. Initialize state s_1 and preprocessed sequenced Φ_1
5. **For** $t = 1, 2, \dots, T$ **do**
6. With probability ϵ select a random action a_t
otherwise select $a_t = \max_a Q(\Phi(s_t), a; \theta)$
7. Execute action at in emulator and observe reward r_t
and image x_{t+1}
8. Set $s_{t+1} = s_t, a_t, x_{t+1}$ and preprocess $\Phi_{t+1} = \Phi(s_{t+1})$
9. Store transition $(\Phi_t, a_t, r_t, \Phi_{t+1})$ in D
10. Sample random minibatch of transitions $(\Phi_j, a_j, r_j, \Phi_{j+1})$
from D
11. Calculate two streams of evaluated deep networks including $V(\Phi(s_j); \theta, \beta_1)$ and $A(\Phi(s_j), a; \theta, \beta_2)$ and combine them as $Q(\Phi(s_j), a; \theta, \beta_1, \beta_2)$ using equation (13)
12. Set $y_j = r_j$ for terminal Φ_{j+1}
otherwise set $y_j = r_j + \gamma \max_{a'} Q(\Phi_{j+1}, a'; \theta)$
13. Perform a gradient descent step on $(y_j - Q(\Phi_j, a_j; \theta))^2$
according to equation 9
14. **end for**
15. **end for**

E. Prioritized Replay DQL

In Common DQL, the sampling of learning is uniform and random, but the learning efficiency could be low in some RL cases. So temporal-difference (TD) error δ is introduced in Prioritized Replay DQL. TD error reflects the difference between the value in the current state and next-step estimate and could be used to measure approximately the amount that the agent can learn from a transition in its current state [23]. TD error δ is calculated as follows:

$$\delta = |r + \gamma \max_{a'} Q(s', a') - Q(s, a)| \quad (16)$$

Then the sample priority is sorted by the value of δ . The higher the priority, the higher the probability of the sample being extracted to learning. The probability of sampling transition i is defined as:

$$P(i) = \frac{p_i^\psi}{\sum_k p_k^\psi} \quad (17)$$

where $p_i > 0$ is the priority of transition i . The exponent ψ determines how much prioritization is used. In proportional prioritization, the expression of p_i is as follows:

$$p_i = |\delta_i| + \varepsilon \quad (18)$$

where ε is a small positive constant. ε is added in the equation (18) to prevent situations that the probability of sampling transition is zero when the TD error is zero.

TABLE IV
IMPLEMENTATION CODE OF PRIORITIZED REPLAY DQL ALGORITHM

Prioritized Replay DQL Algorithm

1. Input: minibatch k , step-size η , replay period K and size N , exponents ψ and λ , budget T .
2. Initialize replay memory H , $\Delta = 0$, $p_1 = 1$
3. Observe S_0 and choose $A_0 \sim \pi_\theta(S_0)$
4. **For** $t = 1, 2, \dots, T$ **do**
5. Observe S_t, R_t, γ_t
6. Store transition $(S_{t-1}, A_{t-1}, R_t, \gamma_t, S_t)$ in H with maximal priority $p_t = \max_{i < t} p_i$
7. **if** $t \equiv 0 \pmod K$ then
8. **For** $j = 1, 2, \dots, k$ **do**
9. Sample transition $j \sim P(j) = p_j^\psi / \sum_i p_i^\psi$
10. Compute importance-sampling weight $\omega_j = (N \cdot P(j))^{-\lambda} / \max_i \omega_i$
11. Compute TD-error δ_j according to equation 16
12. Update transition priority $p_j \leftarrow |\delta_j|$
13. Accumulate weight-change $\Delta \leftarrow \Delta + \omega_j \cdot \delta_j \cdot \nabla_{\theta} Q(S_{j-1}, A_{j-1})$
14. **end for**
15. Update weights $\theta \leftarrow \theta + \eta \cdot \Delta$, reset $\Delta = 0$
16. **end if**
17. Choose action $A_t \sim \pi_\theta(S_t)$
18. **end for**

The stochastic prioritization solves the loss of diversity that may occur when extracting according to the priority, but it also

introduces bias. The bias can be corrected by using importance-sampling (IS) weights:

$$\omega_i = \left(\frac{1}{N} \cdot \frac{1}{P(i)} \right)^\lambda \quad (19)$$

where N is the size of memory and is the exponent. If $\lambda=1$, the non-uniform probabilities can be fully compensated by using $\omega_i \delta_i$ instead of δ_i . Finally, the prioritized replay DQL algorithm is obtained, which can improve the learning speed by optimizing the random sampling process. The implemented code of Prioritized Replay DQL is described in Table IV.

III. DECISION-MAKING PROBLEM ON FREEWAY

In this section, the decision-making problem on the freeway is constructed. First, the freeway driving scenario is constructed, and the training goal is given. Then, the high-level controller for surroundings vehicles based on IDM and MOBIL and the low-level controller for all vehicles are introduced to generate motion command. Furthermore, a kinematic bicycle model is utilized to capture vehicle motion.

A. Freeway Driving Scenario

The decision-making module significantly affects the driving performance of the autonomous vehicle [24]. In this module, the autonomous vehicle needs to select appropriate driving behaviors and generate safe and efficient trajectories to follow.

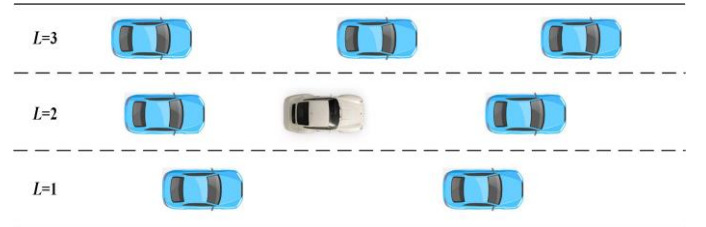


Fig. 2. The freeway driving scenario.

This work chooses a section of the freeway as the driving scenario. On the freeway, common driving behaviors mainly include car-following, lane-changing, and overtaking. The driving scenario is depicted in Fig. 2, wherein the white car is the ego vehicle, and the blue cars represent the surrounding vehicles. In this scenario, the numbers of lanes and the surrounding vehicles are respectively K and N .

The goal of the ego vehicle is to drive at a speed as high as possible without crashing with other vehicles. Besides, the ego vehicle is encouraged to drive on the rightmost lane when not overtaking. Through training, the ego vehicle needs to learn a decision-making strategy, which can reach the driving goal.

In each episode, the original velocity of the ego vehicle and the surrounding vehicles are randomly chosen from [23, 25] m/s and from [20, 23] m/s. The maximum speed is 40m/s, and the length and width of all vehicles are 5m and 2m. The duration of one episode is 100s, but it will immediately terminate when a collision happens.

B. High-level Controller of Surrounding Vehicles

In this paper, the expected speed and target lane of the ego car during each time-step are generated by DRL, while the

motions of the surrounding vehicles are controlled by IDM and MOBIL [25] [26]. IDM is to generate longitude acceleration for car-following without collision, and MOBIL is to give the lane-changing command by evaluating the feasibility and value of the lane-changing intention. The default configuration of the IDM and MOBIL is given in Table V.

IDM is usually utilized to control longitude acceleration for an adaptive cruise controller of autonomous vehicles. According to the relative speed Δv and the relative distance Δd to the front car, the longitude acceleration of the vehicle a is generated as:

$$a = a_{\max} \left[1 - \left(\frac{v}{v_{ex}} \right)^\delta - \left(\frac{d_{ex}}{\Delta d} \right)^2 \right] \quad (20)$$

where v is the longitude speed of the vehicle at this moment. a_{\max} is the maximum acceleration, and δ is the constant acceleration parameter. v_{ex} is the expected speed derived by a_{\max} and d_{ex} . d_{ex} , the expected distance between the vehicle and its front vehicle, is calculated as:

$$d_{ex} = d_0 + Tv + \frac{v\Delta v}{2\sqrt{a_{\max}b}} \quad (21)$$

where d_0 and T are the minimum relative distance and the time interval, which are predefined to ensure safety. b is the deceleration rate to improve driving comfort.

MOBIL determines to change lane when the target lane satisfies both the safety and incentive conditions. The two conditions are respectively as:

$$a_n^{af} \geq -b_{safe} \quad (22)$$

$$a_e^{af} - a_e^{be} + p[(a_n^{af} - a_n^{be}) + (a_o^{af} - a_o^{be})] \geq a_{th} \quad (23)$$

where a_e^{be} , a_o^{be} , a_n^{be} are the accelerations of the vehicle, its follower at the initial lane, its follower at the target lane before lane changing. a_e^{af} , a_o^{af} , a_n^{af} are the accelerations of the vehicle, its follower at the initial lane, its follower at the target lane after lane changing. b_{safe} is the deceleration limit and a_{th} is the acceleration threshold. p is named as the politeness coefficient to meet a trade-off between the vehicle and its followers.

TABLE V

THE DEFAULT CONFIGURATION OF THE IDM AND MOBIL

Symbol	Meaning	Values
a_{\max}	Maximum acceleration	6 m/s ²
δ	Acceleration argument	4
d_0	Minimum relative distance	10 m
T	Safe time gap	1.5 s
b	Comfortable deceleration rate	5 m/s ²
b_{safe}	Safe deceleration limit	2 m/s ²
p	Politeness factor	0.001
a_{th}	Acceleration threshold	0.2 m/s ²

To avoid crash the vehicle that is changing lane, the follower at the target lane may have to decelerate. The safety condition means that the deceleration should not exceed the deceleration limit to ensure safety. The incentive condition requires that the

integrated benefit of the vehicle and its followers' acceleration is bigger than the threshold.

C. Low-level Controller of Vehicles

With the input including reference speed and target lane, the low-level controller translates them into the vehicle acceleration and the steering angle. The vehicle acceleration a is controlled by a proportional controller and calculated as:

$$a = K_p (v_{ex} - v) \quad (24)$$

where K_p is the acceleration control gain, v_{ex} is the expected speed. The controller of steering angle δ is a proportional-derivative controller:

$$v_{ex,lat} = -K_{p,lat} d_{lat} \quad (25)$$

$$\theta_{ex} = \arcsin\left(\frac{v_{ex,lat}}{v}\right) + \theta_L \quad (26)$$

$$\dot{\theta} = K_{p,\theta} (\theta_{ex} - \theta) \quad (27)$$

$$\delta = \arcsin\left(\frac{1}{2} \frac{l_r}{v} \dot{\theta}\right) \quad (28)$$

where $K_{p,lat}$ and $K_{p,\theta}$ are the position and heading control gains, $v_{ex,lat}$ is the expected lateral speed, d_{lat} is the lateral distance between the vehicle and the center-line of the target lane, θ_L is the target lane heading, θ_{ex} is the expected heading, and θ is the current heading.

D. Kinematics of Vehicles

A Kinematic Bicycle Model [27] is utilized in this work for capturing vehicle motion. In the proposed bicycle model, the right and left wheels of the car are combined into a single wheel to describe the vehicle motion, as illustrated in Fig. 3. Besides, this model assumes that only the front wheel can steer, and the wheels have no sliding.

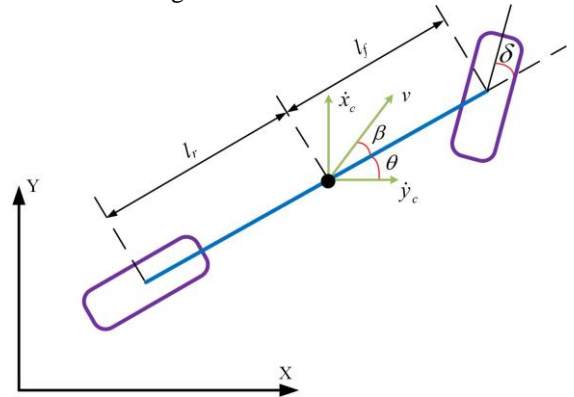


Fig. 3. The kinematic bicycle model.

Two inputs of the model are the steering angle of the front wheel δ and the acceleration a . The motion trajectories of the center of the gravity can be achieved with the input as:

$$\dot{x}_c = v \cos(\theta + \beta) \quad (29)$$

$$\dot{y}_c = v \sin(\theta + \beta) \quad (30)$$

$$a = \dot{v} \quad (31)$$

Different Shapes of Rewards in four DRL Methods

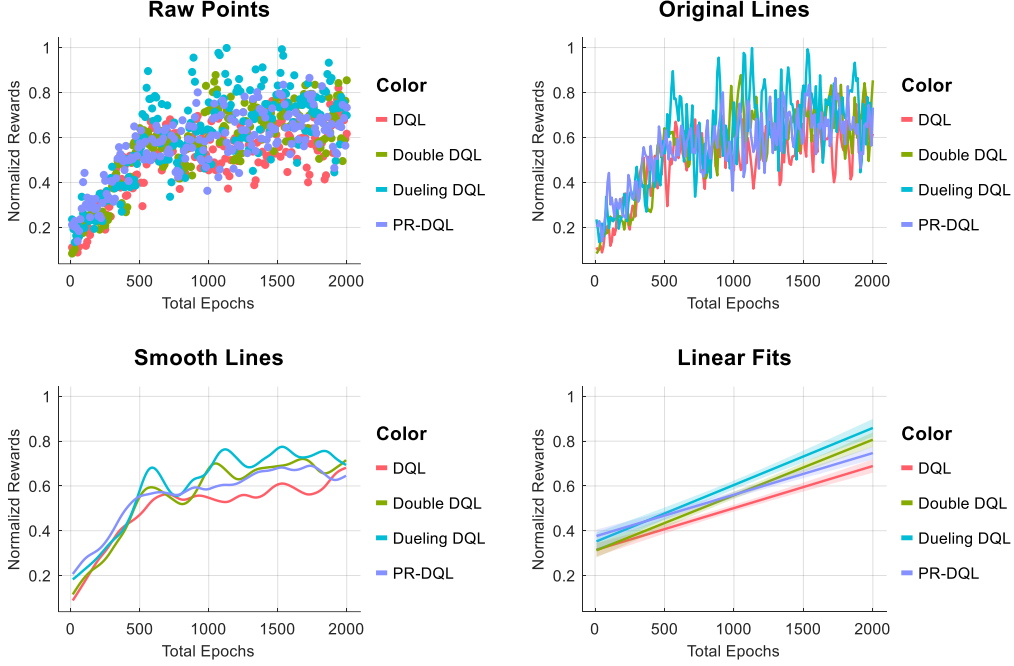


Fig. 4. Normalized reward trajectories in four DRL methods: DQL, Double DQL, Dueling DQL and PR-DQL.

Different Speed Trajectories in four DRL Methods

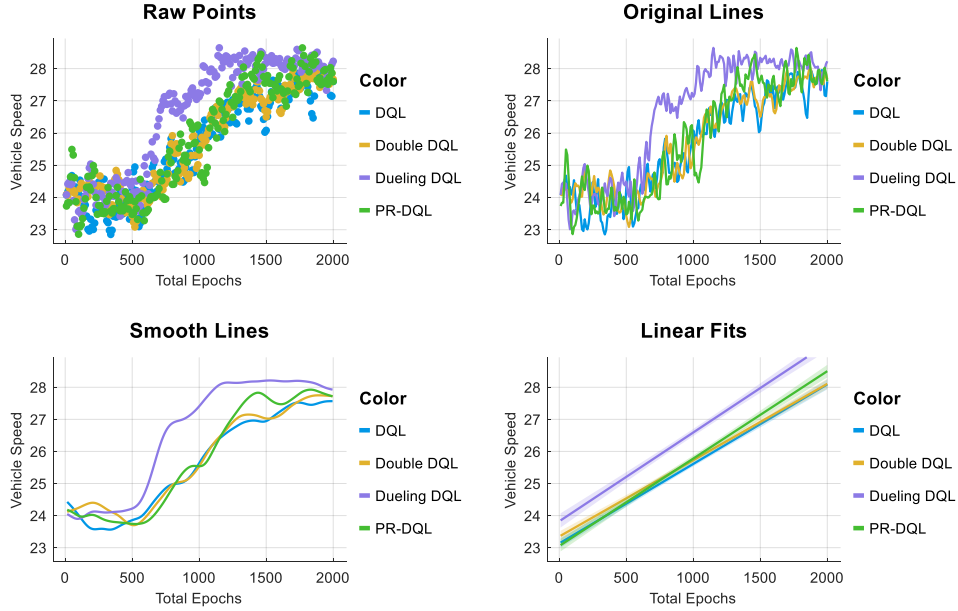


Fig. 5. Average speed curves of the ego vehicle in the four compared DQL algorithms.

$$\dot{\theta} = \frac{v \sin \beta}{l_r + l_f} \quad (32)$$

$$\beta = \tan^{-1} \left(\frac{l_r \tan \delta}{(l_r + l_f)} \right) \quad (33)$$

where (x_c, y_c) is the position of the center of gravity, θ is the heading of the bicycle, β is the slip angle at the center of gravity, l_r is the distance between the center of the front wheel and the center of gravity, l_f is the distance between the center of the rear wheel and the center of gravity. The realization of four

DQL-based decision-making problem is conducted in Python [28] with the highway environment.

IV. EXPERIMENTS AND DISCUSSION

In this section, the simulation results of four DRL methods are discussed and analyzed. First, the learning process of these approaches is compared, including the rewards and state variables. Then, the convergent procedure of DRL algorithms is elaborated. The merits of variations in the DQL technique are given. Finally, an evaluation experiment is conducted to apply these trained decision-making strategies for a similar test.

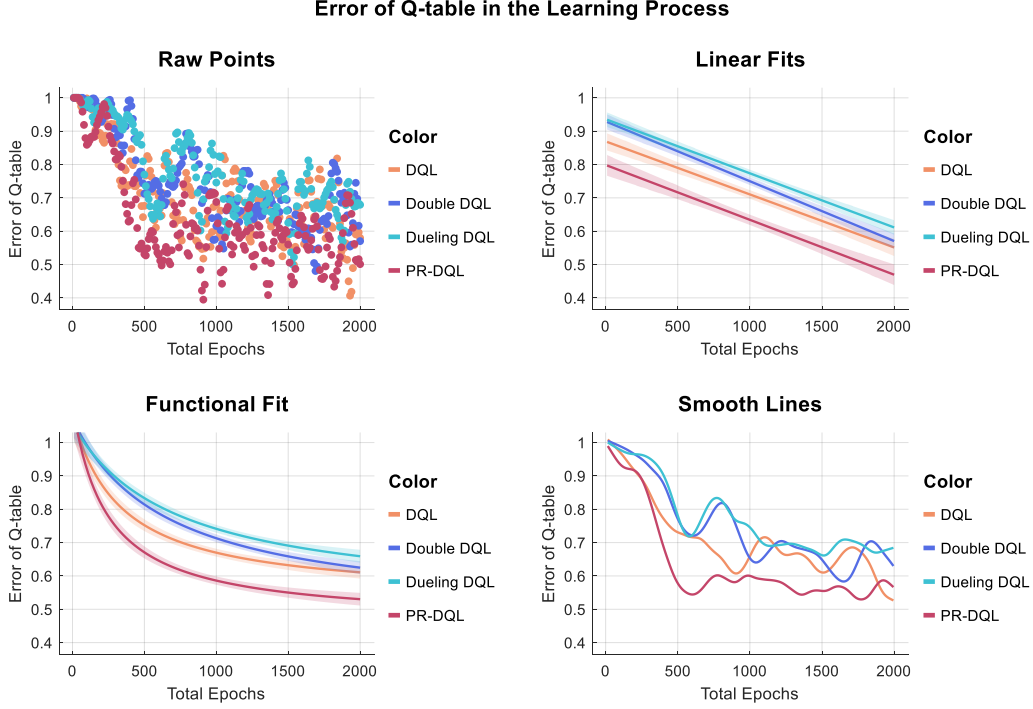


Fig. 7. Error of Q-table in four compared DRL methods to indicate the convergence rate.

A. Learning Process of DRL Methods

For convenience, the approaches introduced in Section II are called DQL, Double DQL, Dueling DQL, and PR-DQL in the following content. The Double DQL algorithm is proposed to avoid the overestimation of the value function. Dueling DQL is constructed to underline the advantage of control action choice. PR-DQL is utilized to improve learning efficiency by increasing the priority of some sample experiences. In these four methods, the parameters set are the same. The total epoch is 2000, and the duration of the driving scenario is 100 (which means the maximum value of the reward is 100). The discount factor γ and learning rate α are 0.8 and 0.2. The lane number is 3, and the number of surrounding vehicles is 15. The reward function is the combination of vehicle speeds and collision conditions.

This subsection explains the learning process of these four algorithms in the freeway decision-making problem. Fig. 4 shows the different types of normalized reward trajectories, including the raw points, original lines, smooth lines, and linear fits. The reward would increase along with episode number. It indicates the ego vehicle becomes more familiar with the driving environments via a trial-and-error procedure. In the cases of smooth lines and linear fits, it is obvious that Dueling DQL has the best performance. Its reward is always higher than the other three methods. Double DQL and PR-DQL have nearly the same effect, which is better than DQL.

The vehicle speed and traveling distance are selected as the state variables in this work. The average speed in these four control cases is depicted in Fig. 5. Since the higher vehicle speed would lead to greater reward, the velocity curves are able to reflect the merits of decision-making policy. Due to the advantage function in Dueling DQL, this algorithm also has the

best control performance. In the other three cases, PR-DQL has a better speed trajectory. Double DQL is the same as DQL.

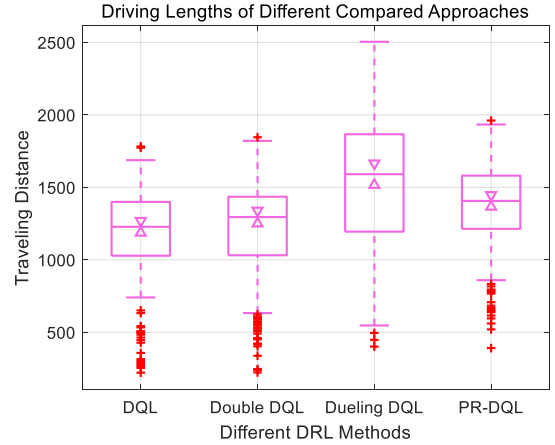


Fig. 6. Traveling distances of the ego vehicle are compared for estimation of control performance.

Furthermore, the traveling distances of the ego vehicle are displayed in Fig. 6. The boxplot figures are used to describe 2000 (episode number is 2000) sample data in each algorithm. It can be discerned that the Dueling DQL has the biggest traveling distance. Moreover, the median of Dueling DQL is also the largest. In this comparison, PR-DQL is better than double DQL and DQL. Thus, it can be observed that the decision-making strategy from Dueling DQL has the best learning efficiency in this freeway problem.

B. Convergent Procedure of DRL Algorithms

This subsection compares the convergence rate of the above four DRL techniques. As described in Section II, the main difference between RL and DRL is applying a neural network to approximate the Q-table. In DQL and PR-DQL, there is only

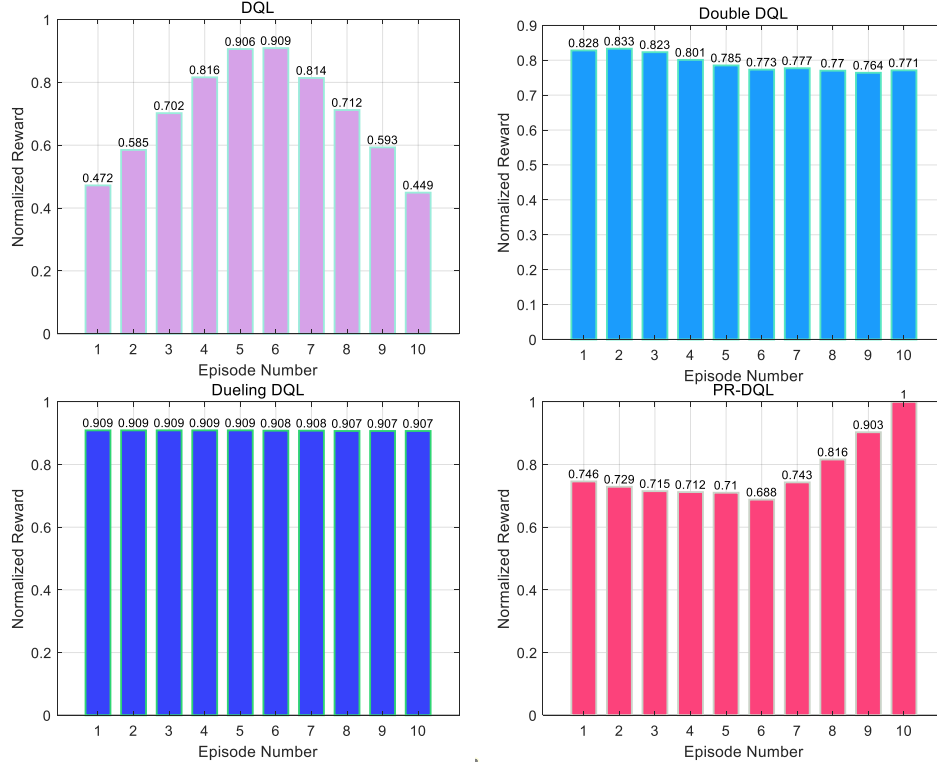


Fig. 9. Normalized values of reward in the testing experiments in four DQL algorithms.

one neural network, but in the other two methods, there are two networks. To express the convergence rate of different DRL algorithms, the mean discrepancy of Q-table and cumulative rewards are often compared.

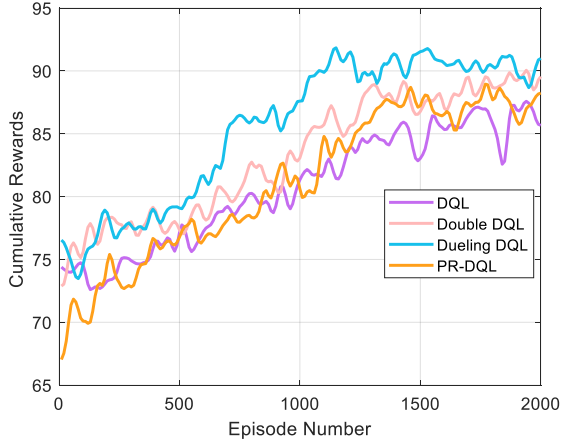


Fig. 8. Accumulated rewards in DQL, Double DQL, Dueling DQL, and PR-DQL.

Fig. 7 describes the four shapes of error of Q-table in these four control cases. The principal impact of the value is the training of neural networks. From the figures of linear fits and functional fit, the PR-DQL has the fastest convergence rate. This is attributed to the chosen rule of sample experiences in PR-DQL. In DQL, there is only one network, and thus DQL is better than Double DQL and Dueling DQL. Furthermore, the convergent procedure of Dueling DQL is slowest. Hence, although the performance of Dueling DQL is best, it consumes the most training time. For different studying problems, the different DRL should be selected (e.g., if the problem does not care about the time, Dueling DQL can be chosen).

Moreover, the accumulated rewards in (1) of different algorithms are given in Fig. 8. It is the sum of the current reward and discounted future rewards. Since the reward is influenced by the control actions, these curves could be utilized to evaluate the decision-making policies. It can be noticed that the values in Dueling DQL are larger than those in the other three methods. Double DQL is almost the same as the PR-DQL. The uptrend of cumulative reward shows the ego vehicle would be familiar with the driving environments. These results also imply that the Dueling DQL algorithm is more compatible with the decision-making problem on the freeway.

C. Testing Experiments for Trained Policies

In this subsection, the trained four decision-making policies are verified in a similar driving scenario. The testing number of episodes is 10. The number of lanes and surrounding vehicles is still 3 and 15. However, the speed and position of these vehicles are always random, and thus the trained strategies need to adapt to this driving situation. According to the values of reward, it can be noticed that the collision happens or not. Thus, we could recognize these decision-making policies can handle the uncertainties or not.

First, the normalized reward in each testing episode is depicted in Fig. 9. Many characteristics can be discerned from this figure. PR-DQL has the maximum value of the reward (reward=1). DQL has the minimum value (reward=0.449), and the rewards in this case are unstable. Double DQL and Dueling DQL are very steady, but Dueling DQL is better than the former. Furthermore, the values of reward in Dueling DQL are nearly the same and very high, which implies that the DRL algorithm is suitable for the decision-making problem on the freeway. In most cases, three variations of DQL are better than the common DQL, which means these changes are necessary.

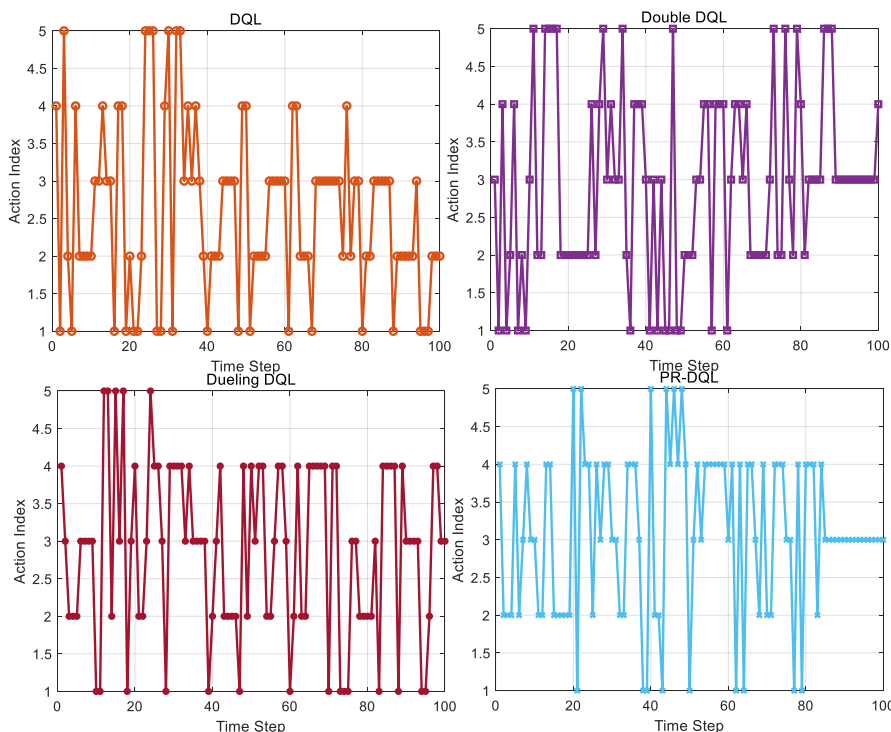


Fig. 10. Control action trajectories from four compared approaches (DQL, Double DQL, Dueling DQL and PR-DQL) in the testing environment.

To indicate the decision-making policies from different methods are not exactly the same. The control actions chosen from four individual episodes are compared in Fig. 10. The episode index in these four techniques in Fig. 9 is 6, 2, 3, and 10, respectively, which indicates the best performance in each method. The control actions are labeled as 5 indexes. They represent the commands of changing left lane, idling speed, changing right lane, running slower, and running faster, respectively. These control actions are different, which means the relevant decision-making policies are different. It leads the differences in control performance and convergence rate. From the above discussion, the Dueling DQL has the best effects in the freeway decision-making problem. However, it has the longest training time. Finally, the suggestion for selecting the DQL algorithm for a similar decision-making problem is: if your studied problem has excellent complexity, the PR-DQL is recommended, otherwise, the Dueling DQL is suggested.

V. CONCLUSION

Four DQL algorithms are compared in the decision-making problem for autonomous vehicles on the freeway. The realization workflows of these four methods are first given. Then, the driving scenario and a bi-level control framework are constructed to regulate the behaviors of the ego vehicle and its surrounding vehicles. Simulation results discussed the learning process, convergence rate, and testing experiments of these four approaches. The choices for DQL algorithms in similar problems depend on the complexity of the research problem. In conclusion, Dueling DQL and PR-DQL are recommended.

Future work includes two aspects. One is applying the decision-making policies in the visualization software. Another is using real-world driving data to assess the property of the derived decision-making strategies.

REFERENCES

- [1] A. Raj, J. A. Kumar, and P. Bansal, "A multicriteria decision making approach to study barriers to the adoption of autonomous vehicles," *Transp. Res. Pt. A-Policy Pract.*, vol. 133, pp. 122-137, 2020.
- [2] J. Tang, S. Liu, S. Pei, S. Zuckerman, C. Liu, and J. Gaudiot, "Teaching autonomous driving using a modular and integrated approach," *arXiv preprint arXiv:1802.09355*, 2018.
- [3] T. Liu, B. Tian, Y. Ai, L. Chen, F. Liu, and D. Cao, "Dynamic States Prediction in Autonomous Vehicles: Comparison of Three Different Methods," in *Proc. 2019 IEEE ITSC*, Auckland, New Zealand, 2019, pp. 3750-3755.
- [4] Q. H. Do, H. Tehrani, S. Mita, M. Egawa, K. Muto, and K. Yoneda, "Human drivers based active-passive model for automated lane change," *IEEE Intell. Transp. Syst. Mag.*, vol. 9, no. 1, pp. 42-56, 2017.
- [5] G. Xiong, Z. Kang, H. Li, W. Song, Y. Jin, and J. Gong, "Decision-making of Lane Change Behavior Based on RCS for Automated Vehicles in the Real Environment," in *Proc. 2018 IEEE IV*, Changshu, China, 2018, pp. 1400-1405.
- [6] K. Shu, H. Yu, X. Chen, L. Chen, Q. Wang, L. Li and D. Cao, "Autonomous Driving at Intersections: A Critical-Turning-Point Approach for Left Turns," *arXiv preprint arXiv:2003.02409*, 2020.
- [7] V. Sezer, "Intelligent decision making for overtaking maneuver using mixed observable Markov decision process," *J. Intell. Transport. Syst.*, vol. 22, no. 3, pp. 201-217, 2017.
- [8] B. Mirchevska, C. Pek, M. Werling, M. Althoff, and J. Boedecker, "High-level decision making for safe and reasonable autonomous lane changing using reinforcement learning," in *Proc. 2018 21st Int. Conf. ITSC*, Hawaii, USA, 2018, pp. 2156-2162.
- [9] J. Duan, S. E. Li, Y. Guan, Q. Sun, and B. Cheng, "Hierarchical reinforcement learning for self-driving decision-making without reliance on labelled driving data," *IET Intell. Transp. Syst.*, vol. 14, no. 5, pp. 297-305, 2020.
- [10] F. Ye, X. Cheng, P. Wang, and C.-Y. Chan, "Automated Lane Change Strategy using Proximal Policy Optimization-based Deep Reinforcement Learning," *arXiv preprint arXiv:2002.02667*, 2020.
- [11] X. Feng, J. Hu, Y. Huo, and Y. Zhang, "Autonomous Lane Change Decision Making Using Different Deep Reinforcement Learning Methods," in *Proc. 19th. CICTP*, Nanjing, China, 2019, pp. 5563-5575.
- [12] T. Liu, B. Huang, Z. Deng, H. Wang, X. Tang, X. Wang and D. Cao, "Heuristics-oriented overtaking decision making for autonomous vehicles using reinforcement learning", *IET Electr. Syst. Transp.*, 2020.

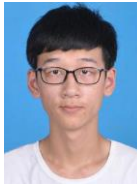
- [13] R. Sutton, and A. Barto, in *Reinforcement learning: An introduction*, 2th ed. Cambridge, Massachusetts, USA:MIT press, 2018.
- [14] T. Liu, X. Hu, W. Hu, Y. Zou, "A heuristic planning reinforcement learning-based energy management for power-split plug-in hybrid electric vehicles," *IEEE Trans. Ind. Inform.*, vol. 15, no. 12, pp. 6436-6445, 2019.
- [15] A. Alizadeh, M. Moghadam, Y. Bicer, N. Ure, U. Yavas, and C. Kurtulus, "Automated Lane Change Decision Making using Deep Reinforcement Learning in Dynamic and Uncertain Highway Environment," in *Proc. 2019 IEEE ITSC*, Auckland, New Zealand, 2019, pp. 1399-1404.
- [16] X. Hu, T. Liu, X. Qi, and M. Barth, "Reinforcement learning for hybrid and plug-in hybrid electric vehicle energy management: Recent advances and prospects," *IEEE Ind. Electron. Mag.*, vol. 13, no. 3, pp. 16-25, 2019.
- [17] T. Liu, X. Tang, H. Wang, H. Yu, and X. Hu, "Adaptive Hierarchical Energy Management Design for a Plug-in Hybrid Electric Vehicle," *IEEE Trans. Veh. Technol.*, vol. 68, no. 12, pp. 11513-11522, 2019.
- [18] T. Liu, B. Wang, and C. Yang, "Online Markov Chain-based energy management for a hybrid tracked vehicle with speedy Q-learning," *Energy*, vol. 160, pp. 544-555, 2018.
- [19] T. De Bruin, in *Sample Efficient Deep Reinforcement Learning for Control*, 2020.
- [20] V. Mnih, K. Kavukcuoglu, D. Silver, A. Graves, I. Antonoglou, D. Wierstra and M. Riedmiller, "Playing atari with deep reinforcement learning," *arXiv preprint arXiv:1312.5602*, 2013.
- [21] H. Van Hasselt, A. Guez, and D. Silver, "Deep reinforcement learning with double q-learning," in *Proc. 30th AAAI-16*, Arizona, USA, 2016, pp. 2094-2100.
- [22] Z. Wang, T. Schaul, M. Hessel, H. Hasselt, M. Lanctot, and N. Freitas, "Dueling network architectures for deep reinforcement learning," in *Proc. Int. conf. machine learning*, New York, USA, 2016, pp. 1995-2003.
- [23] T. Schaul, J. Quan, I. Antonoglou, and D. Silver, "Prioritized experience replay," *arXiv preprint arXiv:1511.05952*, 2015.
- [24] C. Hoel, K. Driggs-Campbell, K. Wolff, L. Laine, and M. J. Kochenderfer, "Combining planning and deep reinforcement learning in tactical decision making for autonomous driving," *IEEE Trans. Intell. Veh.*, vol. 5, no. 2, pp. 294-305, 2019.
- [25] M. Treiber, A. Hennecke, and D. Helbing, "Congested traffic states in empirical observations and microscopic simulations," *Phys. Rev. E*, vol. 62, no. 2, p. 1805, 2000.
- [26] A. Kesting, M. Treiber, and D. Helbing, "General lane-changing model MOBIL for car-following models," *Transp. Res. Record*, vol. 1999, no. 1, pp. 86-94, 2007.
- [27] P. Polack, F. Alché, B. d'Andréa-Novel, and A. de La Fortelle, "The kinematic bicycle model: A consistent model for planning feasible trajectories for autonomous vehicles," in *Proc. 2017 IEEE IV*, California, USA, 2017, pp. 812-818.
- [28] L. Edouard, "An environment for autonomous driving decision-making," <https://github.com/eleurent/highway-env>, *GitHub*, 2018.



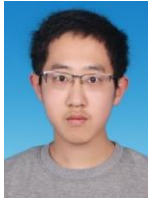
Teng Liu (M'2018) received the B.S. degree in mathematics from Beijing Institute of Technology, Beijing, China, 2011. He received his Ph.D. degree in automotive engineering from Beijing Institute of Technology (BIT), Beijing, in 2017. His Ph.D. dissertation, under the supervision of Pro. Fengchun Sun, was entitled "Reinforcement learning-based energy management for hybrid electric vehicles." He worked as a research fellow in Vehicle Intelligence Pioneers Ltd from 2017 to 2018. Dr. Liu worked as a postdoctoral

fellow at the Department of Mechanical and Mechatronics Engineering, University of Waterloo, Ontario N2L3G1, Canada from 2018 to 2020. Now, he is a member of IEEE VTS, IEEE ITS, IEEE IES, IEEE TEC, and IEEE/CAA. Dr. Liu is now a Professor at the Department of Automotive Engineering, Chongqing University, Chongqing 400044, China. He has more than 8 years' research and working experience in renewable vehicle and connected autonomous vehicle. His current research focuses on reinforcement learning (RL)-based energy management in hybrid electric vehicles, RL-based decision making for autonomous vehicles, and CPSS-based parallel driving. He has published over 40 SCI papers and 15 conference papers in these areas. He received the Merit Student of Beijing in 2011, the Teli Xu Scholarship (Highest Honor) of Beijing Institute of Technology in 2015, "Top 10" in 2018 IEEE VTS Motor Vehicle Challenge and sole outstanding winner in 2018 ABB Intelligent Technology Competition. Dr. Liu is a workshop co-chair in 2018

IEEE Intelligent Vehicles Symposium (IV 2018) and has been reviewer in multiple SCI journals, selectively including IEEE Trans. Industrial Electronics, IEEE Trans. on Intelligent Vehicles, IEEE Trans. Intelligent Transportation Systems, IEEE Transactions on Systems, Man, and Cybernetics: Systems, IEEE Transactions on Industrial Informatics, Advances in Mechanical Engineering.



Bing Huang received the B.S degree in Chongqing University, major in Automotive Engineering. He is currently pursuing M.S. degree in Chongqing University, major in Automotive Engineering. His current research focuses on the decision-making for autonomous driving.



XingYu Mu received the B.S degree in Chongqing University, major in Automotive Engineering. He is currently pursuing M.S. degree in Chongqing University, major in Automotive Engineering. His current research focuses on the left-turn decision-making problem of autonomous driving at intersections.



Fuqing Zhao received the B.S. degree and M.S. degree in University of Science and Technology Beijing, China, major in Materials Engineering. He is currently working in the Comprehensive test center, Chongqing Institute of Green and Intelligent Technology, Chinese Academy of Science. His current research focuses on the vehicle's motion prediction, driving behavior analysis, Dynamic face recognition and the micro/nano fabrication.



Xiaolin Tang received a B.S. in mechanics engineering and an M.S. in vehicle engineering from Chongqing University, China, in 2006 and 2009, respectively. He received a Ph.D. in mechanical engineering from Shanghai Jiao Tong University, China, in 2015. From August 2017 to August 2018, he was a visiting professor of Department of Mechanical and Mechatronics Engineering, University of Waterloo, Waterloo, ON, Canada. He is currently an Associate Professor at the Department of Automotive Engineering, Chongqing University, Chongqing, China. He is also a committeeman of Technical Committee on Vehicle Control and Intelligence of Chinese Association of Automation (CAA). He has led and has been involved in more than 10 research projects, such as National Natural Science Foundation of China, and has published more than 30 papers. His research focuses on Hybrid Electric Vehicles (HEVs), vehicle dynamics, noise and vibration, and transmission control.



Dongpu Cao received the Ph.D. degree from Concordia University, Canada, in 2008. He is currently an Associate Professor and Director of Driver Cognition and Automated Driving (DC-Auto) Lab at University of Waterloo, Canada. His research focuses on vehicle dynamics and control, driver cognition, automated driving and parallel driving, where he has contributed more than 170 publications and 1 US patent. He received the ASME AVTT'2010 Best Paper Award and 2012 SAE Arch T. Colwell Merit Award. Dr. Cao serves as an Associate Editor for IEEE TRANSACTIONS ON VEHICULAR TECHNOLOGY, IEEE TRANSACTIONS ON INTELLIGENT TRANSPORTATION SYSTEMS, IEEE/ASME TRANSACTIONS ON MECHATRONICS, IEEE TRANSACTIONS ON INDUSTRIAL ELECTRONICS and ASME JOURNAL OF DYNAMIC SYSTEMS, MEASUREMENT AND CONTROL. He has been a Guest Editor for VEHICLE SYSTEM DYNAMICS, and IEEE TRANSACTIONS ON SMC: SYSTEMS. He has been serving on the SAE International Vehicle Dynamics Standards Committee and a few ASME, SAE, IEEE technical committees, and serves as the Co-Chair of IEEE ITSS Technical Committee on Cooperative Driving.